Fermi hypernetted-chain calculation of the half-diagonal two-body density matrix of model nuclear matter

M. Petraki and E. Mavrommatis
Physics Department, Division of Nuclear and Particle Physics, University of Athens, Panepistimiopoli, GR-15771 Athens, Greece

J. W. Clark
McDonnell Center for the Space Sciences and Department of Physics, Washington University, St. Louis, Missouri 63130
(Received 22 February 2001; published 25 June 2001)

The half-diagonal two-body density matrix $\rho_{2h}(\mathbf{r}_1,\mathbf{r}_2,\mathbf{r}_{1'})$ is a key quantity in theoretical descriptions of nucleon knockout reactions at intermediate energies, due to its central role in treatments of the propagation and final-state interactions of ejected nucleons in the nuclear medium. This quantity is calculated for a simple model of the ground state of infinite symmetrical nuclear matter, based on a Jastrow-correlated wave function and a Fermi hypernetted-chain analysis. The dependence of ρ_{2h} on the variables $r_{11'}=|\mathbf{r}_1-\mathbf{r}_{1'}|$, $r_{12}=|\mathbf{r}_1-\mathbf{r}_2|$, and the angle θ between $\mathbf{r}_1-\mathbf{r}_{1'}$ and $\mathbf{r}_1-\mathbf{r}_2$ is investigated in some detail. Significant departures from ideal Fermi gas behavior in certain domains reflect the importance of short-range correlations and their interplay with statistical correlations. The quality of approximations to ρ_{2h} proposed by Gersch *et al.*, Rinat, and Silver is assessed by comparison with the Fermi hypernetted-chain results.

DOI: 10.1103/PhysRevC.64.024301 PACS number(s): 21.65.+f, 24.10.Cn, 25.30.Fj

I. INTRODUCTION

In this paper we present results of a numerical calculation of the half-diagonal two-body density matrix $\rho_{2h}(\mathbf{r}_1,\mathbf{r}_2,\mathbf{r}_{1'})$ of the ground state of uniform, isospin symmetrical, spin-saturated nuclear matter. The calculation has been performed within the framework of the microscopic analysis of ρ_{2h} carried out by Ristig and Clark (RC) [1] for a uniform strongly interacting Fermi fluid. The RC analysis implements correlated-basis-function theory at the variational level and exploits hypernetted-chain techniques. The Fourier-space counterpart of ρ_{2h}, known as the generalized momentum distribution $n(\mathbf{p},\mathbf{Q})$, has been the subject of a previous numerical study [2,3] of the nuclear-matter ground state within the same framework.

For a unit-normalized ground-state vector $|\Psi\rangle$, the half-diagonal two-body density matrix is defined by

$$\rho_{2h}(\mathbf{r}_1,\mathbf{r}_2,\mathbf{r}_{1'})=A(A-1)\int \Psi^*(\mathbf{r}_1,\mathbf{r}_2,\mathbf{r}_3,\ldots,\mathbf{r}_A)\Psi(\mathbf{r}_{1'},\mathbf{r}_2,\mathbf{r}_3,\ldots,\mathbf{r}_A)d\mathbf{r}_3\ldots d\mathbf{r}_A. \tag{1}$$

In writing this expression, we have supressed spin/isospin state labels and a sum over all the spin/isospin variables. The system is considered to have constant nucleon density ρ with corresponding Fermi wave number $k_F=(6\pi^2\rho/\nu)^{1/3}$, where $\nu=4$ is the level degeneracy of plane-wave single-particle states. Performing a Fourier transformation in the variables $\mathbf{r}_{11'}=\mathbf{r}_1-\mathbf{r}_{1'}$ and $\mathbf{r}_{1'2}=\mathbf{r}_{1'}-\mathbf{r}_2$, we obtain the generalized momentum distribution

$$n(\mathbf{p},\mathbf{Q})=\frac{1}{\nu}\frac{\rho}{A}\int \rho_{2h}(\mathbf{r}_1,\mathbf{r}_2,\mathbf{r}_{1'})e^{-i\mathbf{p}\cdot(\mathbf{r}_1-\mathbf{r}_{1'})}e^{-i\mathbf{Q}\cdot(\mathbf{r}_{1'}-\mathbf{r}_2)}d\mathbf{r}_1 d\mathbf{r}_2 d\mathbf{r}_{1'}. \tag{2}$$

If dynamical correlations are neglected, the remaining kinematical correlations generated by the Pauli exclusion principle lead to the following half-diagonal two-body density matrix of the infinite noninteracting Fermi system (the ideal Fermi gas)

$$\rho^F_{2h}(\mathbf{r}_1,\mathbf{r}_2,\mathbf{r}_{1'})=\rho\rho^F_1(\mathbf{r}_1,\mathbf{r}_{1'})-\frac{1}{\nu}\rho^F_1(\mathbf{r}_1,\mathbf{r}_2)\rho^F_1(\mathbf{r}_{1'},\mathbf{r}_2). \tag{3}$$

In this expression, $\rho^F_1(\mathbf{r}_i,\mathbf{r}_j)$ is the one-body density matrix of the ideal Fermi gas, given by

$$\rho^F_1(\mathbf{r}_i,\mathbf{r}_j)=\rho l(k_F r_{ij}), \tag{4}$$

in terms of the Slater exchange function $l(x)\equiv 3x^{-3}(\sin x - x\cos x)$, where $r_{ij}=|\mathbf{r}_i-\mathbf{r}_j|$.

Considering the general case where the fermion constituents may experience strong interactions, the half-diagonal two-body density matrix $\rho_{2h}(\mathbf{r}_1,\mathbf{r}_2,\mathbf{r}_{1'})$ of an infinite many-fermion system has several formal properties that are important to our treatment. First, ρ_{2h} is a symmetrical function of $\mathbf{r}_1$ and $\mathbf{r}_{1'}$. Second, with our normalization choice, its diagonal part is related to the radial distribution function $g(r_{12})$ by

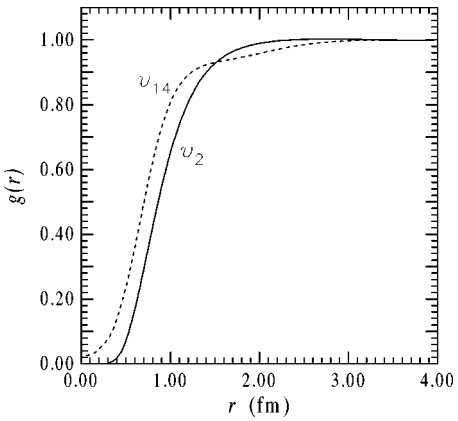

FIG. 1. Radial distribution function $g(r)$ as a function of r. The curve labeled v_2 corresponds to our calculation using MC model [Eq. (15)] and the FHNC/0 algorithm, and curve v_{14} to the variational calculation of Ref. [11] using the Urbana v_{14} potential at $k_F = 1.33$ fm^{-1}.

$$\rho_2(\mathbf{r}_1,\mathbf{r}_2,\mathbf{r}_1) = \rho^2 g(r_{12}). \tag{5}$$

Third, it fulfills the sequential relation

$$\int \rho_{2h}(\mathbf{r}_1,\mathbf{r}_2,\mathbf{r}_{1'})d\mathbf{r}_2 = (A-1)\rho_1(\mathbf{r}_1,\mathbf{r}_{1'}). \tag{6}$$

Fourth, if the system is subject to strong short-range repulsions or has statistical correlations corresponding to single-particle level degeneracy $\nu=1$, the ''hard-core'' condition

$$\rho_{2h}(\mathbf{r}_1,\mathbf{r}_1,\mathbf{r}_{1'}) = 0 \tag{7}$$

must hold. Finally, ρ_{2h} has the asymptotic behavior

$$\lim_{r_2\to\infty} \rho_{2h}(\mathbf{r}_1,\mathbf{r}_2,\mathbf{r}_{1'}) = \rho\rho_1(\mathbf{r}_1,\mathbf{r}_{1'}). \tag{8}$$

Three approximations have been proposed for estimating the half-diagonal two-body density matrix $\rho_{2h}(\mathbf{r}_1,\mathbf{r}_1,\mathbf{r}_{1'})$ of a uniform quantum fluid in terms of the one-body density matrix $\rho_1(\mathbf{r}_1,\mathbf{r}_{1'})$ and the radial distribution function $g(r)$:

(i) Approximation of Gersch, Rodriguez, and Smith [4]

$$\rho^G_{2h}(\mathbf{r}_1,\mathbf{r}_2,\mathbf{r}_{1'}) = \rho\rho_1(\mathbf{r}_1,\mathbf{r}_{1'})[g(r_{12})]^{1/2}[g(r_{1'2})]^{1/2}, \tag{9}$$

(ii) Silver's approximation [5]

$$\rho^S_{2h}(\mathbf{r}_1,\mathbf{r}_2,\mathbf{r}_{1'}) = \rho\rho_1(\mathbf{r}_1,\mathbf{r}_{1'})g(r_{12}), \tag{10}$$

(iii) Rinat's approximation [6]

$$\rho^R_{2h}(\mathbf{r}_1,\mathbf{r}_2,\mathbf{r}_{1'}) = \rho\rho_1(\mathbf{r}_1,\mathbf{r}_{1'})g(|(\mathbf{r}_1+\mathbf{r}_{1'})/2-\mathbf{r}_2|). \tag{11}$$

We note that Silver's approximation lacks symmetry in the variables $\mathbf{r}_1$ and $\mathbf{r}_{1'}$, while Rinat's estimate deviates from the requisite short-range behavior [Eq. (7)]. Otherwise, these approximations fulfill the formal properties of ρ_{2h} listed above.

The three approximations were introduced in the context of deep-inelastic neutron scattering in liquid helium. Among these constructions, those of Gersch *et al.* and Silver have been employed in the analysis of quasielastic electron scattering off nuclei in Refs. [7] and [8], respectively.

The diagonal part of $\rho_{2h}(\mathbf{r}_1,\mathbf{r}_2,\mathbf{r}_{1'})$, which is the radial distribution function $g(r_{12})$ multiplied by ρ^2, can be taken as a minimal descriptor of nucleon-nucleon correlations within the nuclear medium. It has been extensively studied in the case of infinite nuclear matter by means of *ab initio* nuclear many-body theory (for treatments within the variational correlated-basis-function theory, see [9–11]). Its experimental determination in the case of finite nuclei is indirect, but has been attempted in a few cases (for example [12]). By its definition, the half-diagonal two-body density matrix $\rho_{2h}(\mathbf{r}_1,\mathbf{r}_2,\mathbf{r}_{1'})$ is a more detailed descriptor of the correlation structure of the nuclear medium. In analogy with Bose fluids [13,14], this quantity is expected to appear in fundamental sum rules that furnish insights into the nature of the elementary excitations of nuclear matter. Moreover, ρ_{2h} arises naturally in the description of a number of processes occurring in finite nuclei, for example in the calculation of dispersive effects in inelastic electron scattering [15]. However, the growing interest in the half-diagonal two-body density matrix has been largely driven by its appearance in a number of quantitative ''post-mean-field'' treatments of the propagation of ejected nucleons and their final-state interactions (FSI) (see, for example, Refs. [16,7]). A proper account of FSI is critical to the extraction of reliable information on momentum distributions, spectral functions, and transparency of finite nuclei from the results of diverse experiments, notably: (i) inclusive quasielastic (e,e') scattering [17–19], (ii) exclusive $(e,e'N)$ [20–25] and $(e,e'NN)$ [25–27] reactions, (iii) (p,p') and $(p,2p)$ proton scattering and knockout [28,29], and (iv) photonuclear reactions such as (γ,N) [30–33] and $(\gamma,2N)$ [31,34].

The first microscopic theoretical studies of the quantities $n(\mathbf{p},\mathbf{Q})$ and $\rho_{2h}(\mathbf{r}_1,\mathbf{r}_2,\mathbf{r}_{1'})$ in strongly correlated systems were carried out by Ristig and Clark at the variational level of correlated-basis-function theory [1,35]. Starting from cluster-diagrammatic decompositions of these quantities, Ristig and Clark applied hypernetted-chain techniques [9] to their evaluation for a ground-state wave function of Jastrow-Slater or Jastrow form, under the assumption of Fermi or Bose statistics, respectively. In the present work, we report results of a Fermi hypernetted-chain (FHNC) treatment of $\rho_{2h}(\mathbf{r}_1,\mathbf{r}_2,\mathbf{r}_{1'})$ for a simple model of nuclear matter in the leading approximation FHNC/0 defined by the omission of elementary diagrams. The calculational scheme adopted is outlined in Sec. II. In Sec. III, we exhibit and discuss the corresponding numerical results. Section IV presents numerical results for ρ_{2h} in the approximations of Gersch *et al.*, Silver, and Rinat, obtained upon employing the FHNC/0 algorithm to calculate the building blocks $\rho(r_{11'})$ and $g(r)$ of these estimates, which are compared with the FHNC/0 results from our direct calculation of ρ_{2h}. Section V reviews the main conclusions of this investigation and surveys the prospects for future developments.

II. FERMI HYPERNETTED-CHAIN CALCULATION

The RC analysis [1] of the half-diagonal two-body density matrix ρ_{2h} of a uniform, isotropic fluid of A strongly inter-

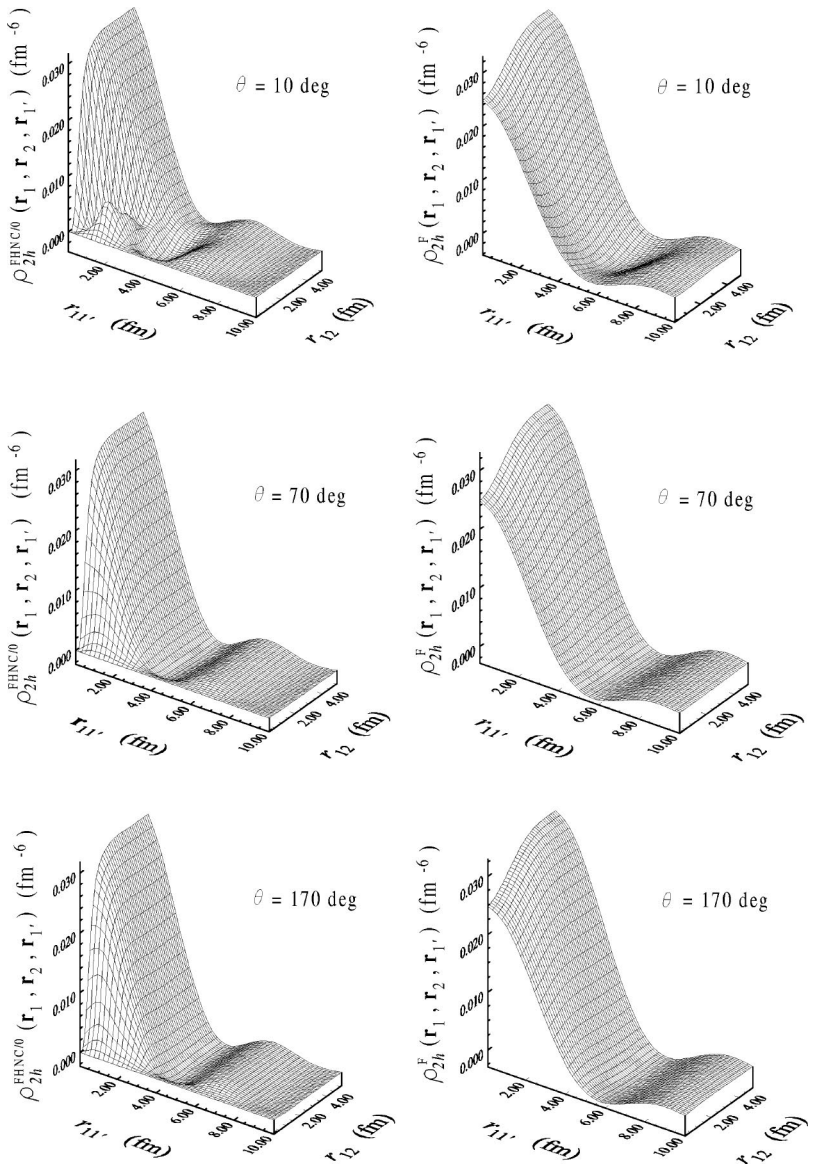

FIG. 2. Half-diagonal two-body density matrix $\rho_{2h}(\mathbf{r}_1,\mathbf{r}_2,\mathbf{r}_{1'})$ for the MC model of uniform symmetrical nuclear matter as given by the FHNC/0 approximation and for the ideal Fermi gas of the same density $\rho=0.182$ fm^{-3}, as a function of r_{12} and $r_{11'}$ for three representative values of $\theta\equiv\widehat{(\mathbf{r}_{11'},\mathbf{r}_{12})}$.

acting fermions in its ground state is predicated on a Jastrow-Slater wave function

$$\Psi=\mathcal{N}^{-1}\prod_{i<j}^{A} f(r_{ij})\Phi. \tag{12}$$

In this ansatz, Φ is a Slater determinant of plane-wave orbitals, representing the ground state of the reference ideal Fermi gas of particle density $\rho=\nu k_F^3/6\pi^2$, while $f(r_{ij})$ is a Jastrow two-body correlation function depending only on the scalar separation of particles i,j. The constant $\mathcal{N}$, taken as the norm of $\Pi f\Phi$, is introduced to normalize Ψ to unity. Development of the corresponding generalized momentum distribution $n(\mathbf{p},\mathbf{Q})$ in a factorized Iwamoto-Yamada cluster expansion leads, in the thermodynamic limit, to an infinite series whose addends are generally reducible, in that they are represented as products of cluster diagrams. Transformation to coordinate space yields the corresponding cluster series for ρ_{2h}. With guidance from analogies with the earlier analysis of the Bose problem [35], resummation of the latter series is then carried out using hypernetted-chain techniques, taking proper account of asymptotic behaviors. The function ρ_{2h} is expressed as a sum of two components, i.e.,

$$\rho_{2h}(\mathbf{r}_1,\mathbf{r}_2,\mathbf{r}_{1'})=\rho_{2h}^{(2)}(\mathbf{r}_1,\mathbf{r}_2,\mathbf{r}_{1'})+\rho_{2h}^{(3)}(\mathbf{r}_1,\mathbf{r}_2,\mathbf{r}_{1'}), \tag{13}$$

where $\rho_{2h}^{(2)}$ contains all terms generated purely by two-point functions, and $\rho_{2h}^{(3)}$ is a remainder whose terms depend also on irreducible three-point functions. (''Two-point'' and ''three-point'' refer to the underlying graphical topology.) The first component, constructed from certain one-body den-

sity matrices and quantities provided by solution of a set of FHNC equations, takes the explicit form

$$\rho_{2h}^{(2)}(\mathbf{r}_1,\mathbf{r}_2,\mathbf{r}_{1'}) = \rho\rho_1(r_{11'})g_{Qdd}(r_{12})g_{Qdd}(r_{1'2}) + \rho\rho_{1D}(r_{11'})l(k_F r_{11'}) \times [g_{Qdd}(r_{12})F_{Qde}(r_{1'2}) + g_{Qdd}(r_{1'2})F_{Qde}(r_{12})] - \nu\rho\rho_{1D}(r_{11'}) \times [\nu^{-1}l(k_F r_{12}) - F_{Qcc}(r_{12})] \times [\nu^{-1}l(k_F r_{1'2}) - F_{Qcc}(r_{1'2})]. \quad (14)$$

The corresponding result for $\rho_{2h}^{(3)}$ may be found in Ref. [1]. [The Q index appearing in Eq. (14) is introduced to make the necessary connection with Ristig's notation [36]; it should not be confused with the momentum variable Q in the definition of the generalized momentum distribution.] Further, $\rho_1(\mathbf{r}_1,\mathbf{r}_{1'})$ is the full one-body density matrix, $\rho_{1D}(\mathbf{r}_1,\mathbf{r}_{1'})$ is its direct-direct (dd) component, the functions $F_{Qxy}(r)$ [with $xy=dd$ (direct-direct), de (direct-exchange), and cc (circular-circular)] are two-point quantities that serve as form factors, and $g_{Qdd}(r)=1+F_{Qdd}(r)$.

The FHNC result for ρ_{2h} may be assembled from diagram sets that are summed in the FHNC treatments of the one-body density matrix [36,37] and the radial distribution function [9]. For example, one has $F_{Qxy}(r)=N_{Qxy}(r)+X_{Qxy}(r)$, where N_{Qxy} and X_{Qxy} are made up of the nodal (N) and the non-nodal (X) diagrams that arise in the FHNC analysis of the one-body density matrix. Here we implement the FHNC algorithm at the initial (zeroth) level where elementary diagrams are omitted, resulting in the so-called FHNC/0 approximation. Contributions from elementary diagrams are expected to become important only at densities higher than ordinarily found in nuclei [38], since they become significant only if three or more particles are close together. We also choose to omit the three-point quantity $\rho_{2h}^{(3)}$, since by similar reasoning it is expected to be small compared to $\rho_{2h}^{(2)}$. This calculational scheme (viz., the FHNC/0 algorithm together with neglect of $\rho_{2h}^{(3)}$) does obey the condition (7), and it preserves the symmetry with respect to $\mathbf{r}_1$ and $\mathbf{r}_{1'}$. However, it is generally accompanied by (relatively small) violations of the diagonal property (5) and the sequential relation (6) [3]. Henceforth, we shall refer to our calculational scheme as FHNC/0 for brevity, and the corresponding estimate of $\rho_{2h}(\mathbf{r}_1,\mathbf{r}_2,\mathbf{r}_{1'})$ will be denoted by $\rho_{2h}^{\mathrm{FHNC/0}}(\mathbf{r}_1,\mathbf{r}_2,\mathbf{r}_{1'})$.

III. NUMERICAL RESULTS

The numerical results for the half-diagonal two-body density matrix $\rho_{2h}^{\mathrm{FHNC/0}}(\mathbf{r}_1,\mathbf{r}_2,\mathbf{r}_{1'})$ are based on a simple model of symmetrical nuclear matter near its saturation density, namely the ''Monte Carlo'' (MC) model [39,40]. This model corresponds to the nucleon density $\rho=0.182$ fm^{-3} (or $k_F=1.392$ fm^{-1}) and is defined by the Jastrow two-body correlation function

$$f(r)=\exp\left[-C_1 e^{-C_2 r}\frac{(1-e^{r/C_3})}{r}\right], \quad (15)$$

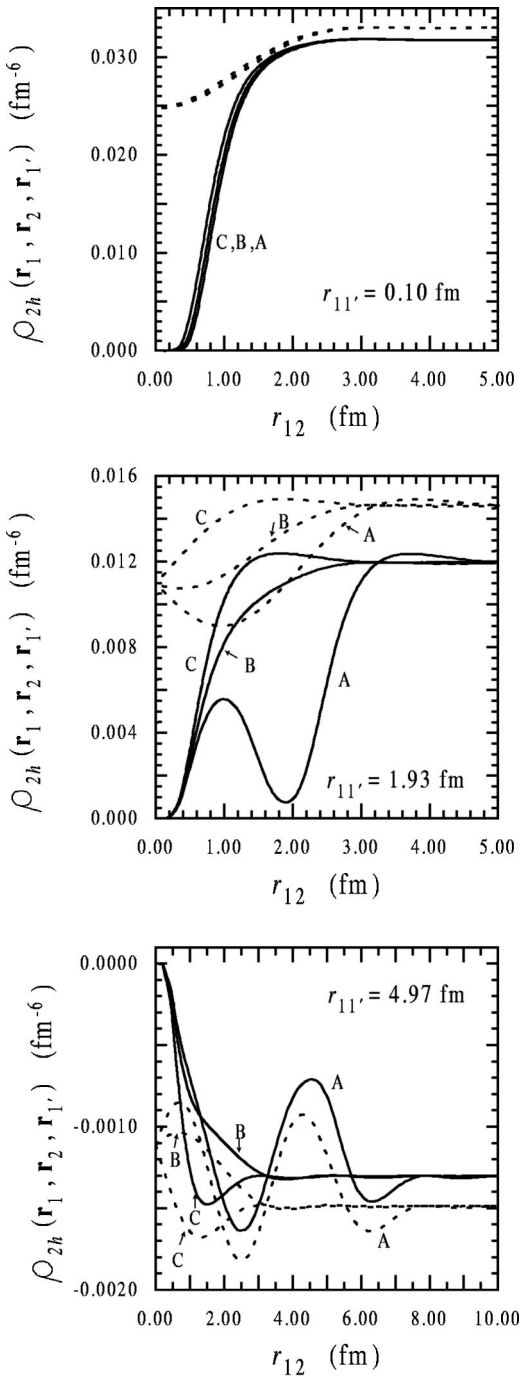

FIG. 3. Half-diagonal two-body density matrix $\rho_{2h}(\mathbf{r}_1,\mathbf{r}_2,\mathbf{r}_{1'})$ at nucleon density $\rho=0.182$ fm^{-3} as a function of r_{12} for constant values of $r_{11'}$ (equal to 0.10, 1.93, and 4.97 fm) and of $\theta \equiv \widehat{(\mathbf{r}_{11'},\mathbf{r}_{12})}$ [equal to 10° (curves A), 70° (curves B), and 170° (curves C)]. Dashed line: ideal Fermi gas. Solid line: FHNC/0 approximation calculated with MC correlations [Eq. (15)].

with parameter values $C_1=1.7$ fm, $C_2=1.6$ fm^{-1}, and $C_3=0.1$ fm. The MC model originated in a variational Monte Carlo treatment of the ground state of symmetrical nuclear matter based on the v_2 potential [41]. The correlation function (15) provides a reasonable ''average'' description of the short-range (and longer-range) spatial correlations, but it

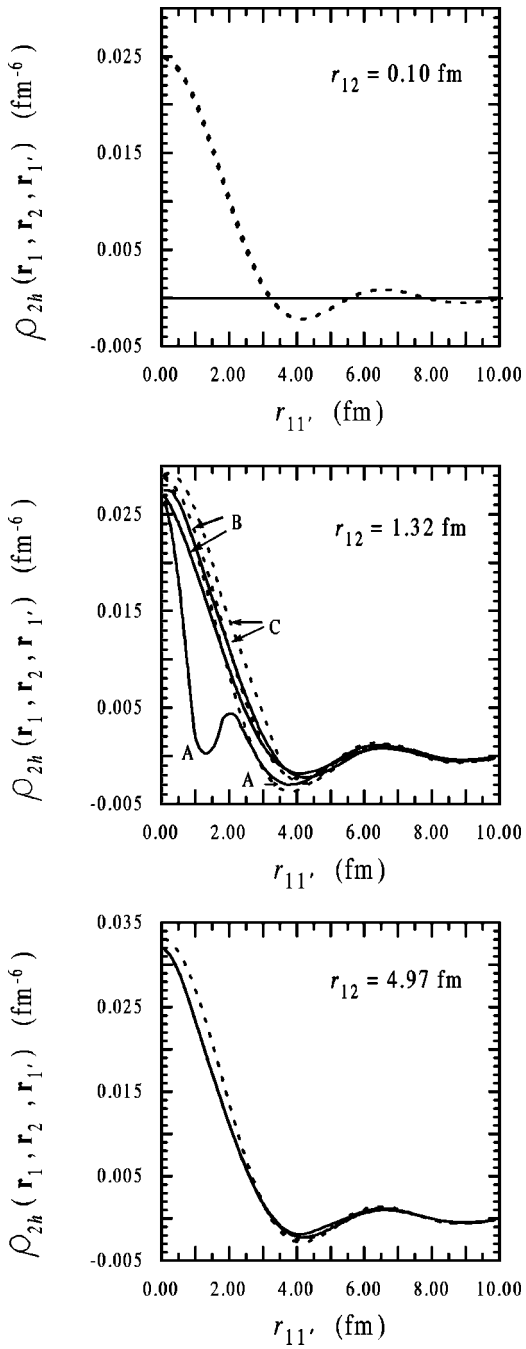

FIG. 4. Half-diagonal two-body density matrix $\rho_{2h}(\mathbf{r}_1,\mathbf{r}_2,\mathbf{r}_{1'})$ at nucleon density $\rho=0.182$ fm^{-3} as a function of $r_{11'}$ for constant values of r_{12} (equal to 0.10, 1.32, and 4.97 fm) and of $\theta \equiv \widehat{(\mathbf{r}_{11'},\mathbf{r}_{12})}$ [equal to 10° (curves A), 70° (curves B), and 170° (curves C)]. Dashed line: ideal Fermi gas. Solid line: FHNC/0 approximation calculated with MC correlations [Eq. (15)]. (For $r_{12}=0.10$ fm and for $r_{12}=4.97$ fm, the FHNC/0 curves are essentially indistinguishable; the same holds for the ideal Fermi gas curves.)

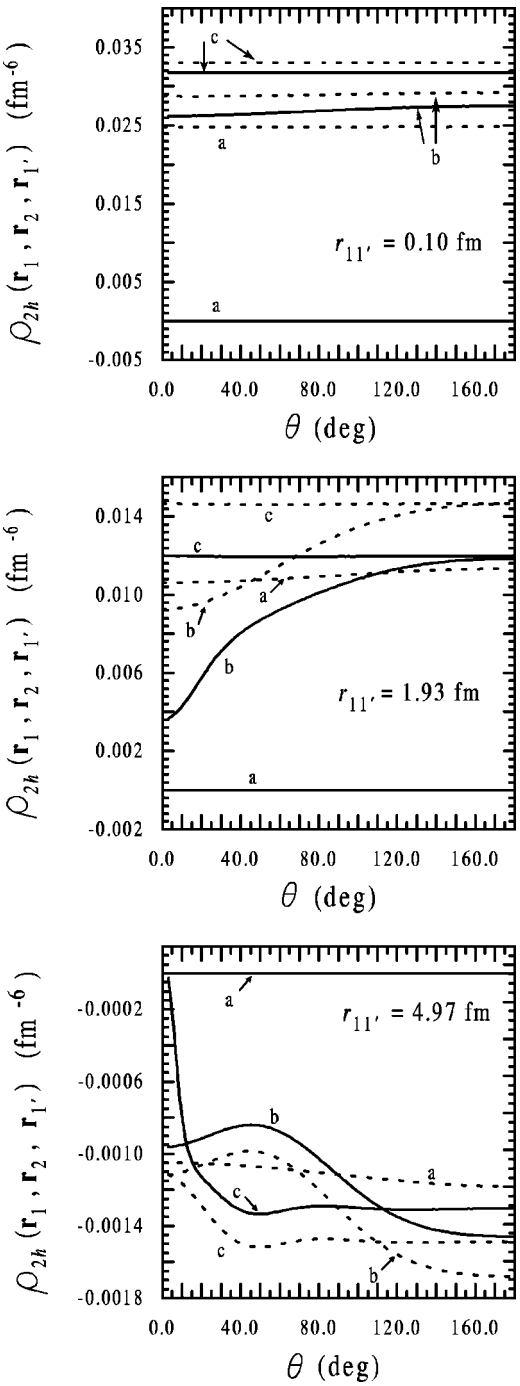

FIG. 5. Half-diagonal two-body density matrix $\rho_{2h}(\mathbf{r}_1,\mathbf{r}_2,\mathbf{r}_{1'})$ at nucleon density $\rho=0.182$ fm^{-3} as a function of $\theta \equiv \widehat{(\mathbf{r}_{11'},\mathbf{r}_{12})}$ for constant values of $r_{11'}$ [equal to 0.10, 1.93, and 4.97 fm] and of r_{12} (equal to 0.10 fm [curves (a)], 1.32 fm [curves (b)], and 4.97 fm [curves (c)]). Dashed line: ideal Fermi gas. Solid line: FHNC/0 approximation calculated with MC correlations [Eq. (15)].

misses the specific effects arising from the state dependence of the realistic nucleon-nucleon interaction.

In Fig. 1, the radial distribution function $g(r)$ derived from the MC model via the FHNC/0 algorithm is compared with the result for $g(r)$ obtained in the chain-summation evaluation [38] reported in Ref. [11], based on the Urbana v_{14} two-nucleon potential and the Urbana-VII three-nucleon interaction. As seen in the figure, the MC model has a larger correlation hole than that produced by the v_{14}/Urbana-VII interaction, reflecting the unrealistically large repulsive core of the v_2 potential. The strength of the two-body correlations

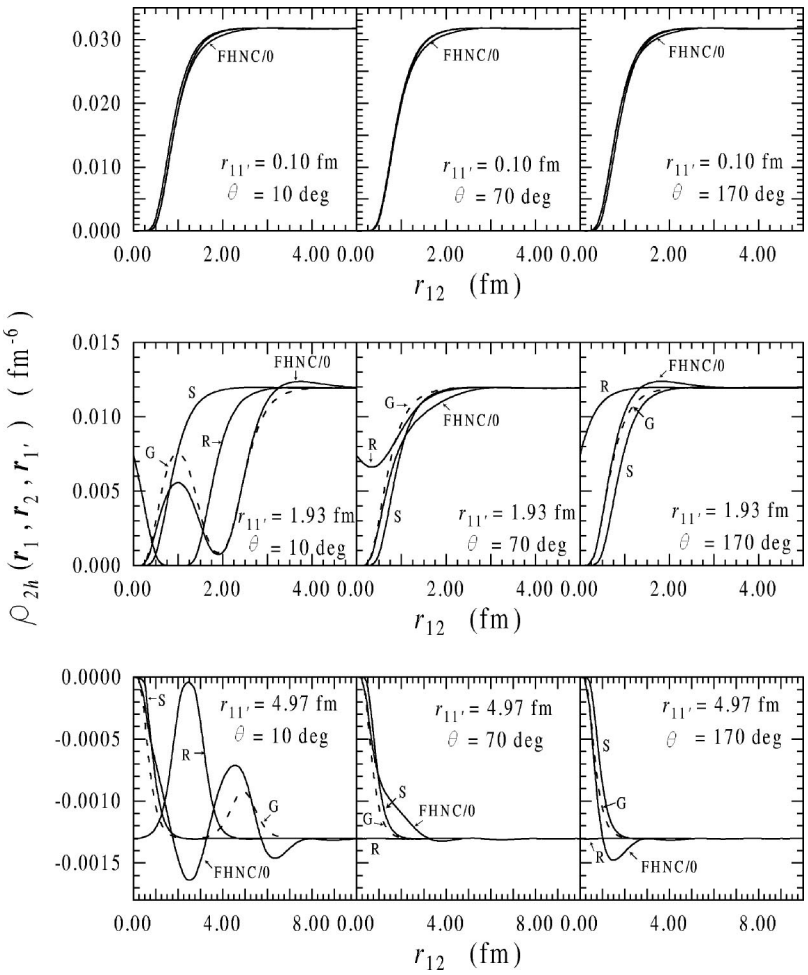

FIG. 6. Approximations $\rho_{2h}^{G}(\mathbf{r}_1,\mathbf{r}_2,\mathbf{r}_{1'})$ (dashed line G), $\rho_{2h}^{S}(\mathbf{r}_1,\mathbf{r}_2,\mathbf{r}_{1'})$ (solid line S), $\rho_{2h}^{R}(\mathbf{r}_1,\mathbf{r}_2,\mathbf{r}_{1'})$ (solid line R), and $\rho_{2h}^{\mathrm{FHNC/0}}(\mathbf{r}_1,\mathbf{r}_2,\mathbf{r}_{1'})$ (solid line FHNC/0), for the MC model of uniform symmetrical nuclear matter, as functions of r_{12}, for representative values of $r_{11'}$ and $\theta \equiv \widehat{(\mathbf{r}_{11'},\mathbf{r}_{12})}$. (For $r_{11'}=0.10$ fm, curves G, S, and R are essentially indistinguishable.)

may be measured by the wound parameter $\kappa_{\mathrm{dir}}=\rho\int[f(r)-1]^2 d\mathbf{r}$, which takes the value 0.297 in the MC model. (Obviously, the corresponding parameter for the v_{14}/Urbana-VII interaction would be significantly smaller.) The MC model, along with another simple model in which $f(r)-1$ has Gaussian shape (the G2 model, with $\kappa_{\mathrm{dir}}=0.111$ at $k_F=1.392$ fm^{-1}), has been employed in previous FHNC/0 calculations of $n(\mathbf{p},\mathbf{Q})$ [2,3]. In contrast to the MC case, the Gaussian or G2 model corresponds to an unrealistically *soft* short-range repulsion. Of the two simple models of the two-body correlations, the MC model appears on balance to be the better choice. While its use may be expected to yield overestimates of the effects of short-range geometric correlations on the two-body density matrix, this feature is actually of advantage in numerical exploration, since it provides for a stronger test of the adequacy of proposed approximations to ρ_{2h}.

We have studied the dependence of $\rho_{2h}^{\mathrm{FHNC/0}}(\mathbf{r}_1,\mathbf{r}_2,\mathbf{r}_{1'})$ on the variables $r_{11'}$, r_{12}, and $\theta \equiv \widehat{(\mathbf{r}_{11'},\mathbf{r}_{12})}$ in the ranges $0 \leqslant r_{11'} \leqslant 10$ fm, $0 \leqslant r_{12} \leqslant 10$ fm, and $0 \leqslant \theta \leqslant 180°$. The three-dimensional plots of Fig. 2 provide representative views of $\rho_{2h}(\mathbf{r}_1,\mathbf{r}_2,\mathbf{r}_{1'})$ as given by the FHNC/0 approximation in juxtaposition with the results for the ideal Fermi gas at the same angles θ and the same density. Figures 3, 4, and 5 display cross sections of the FHNC/0 and Fermi-gas results for the half-diagonal two-body density matrix under variation of one of the three variables $r_{11'}$, r_{12}, and θ, with each of the other two variables kept fixed at three selected values. Since ρ_{2h} is symmetric under interchange of r_{12} and $r_{1'2}$, further information on the behavior of this function may be inferred from the figures provided.

Upon considering the variation of $\rho_{2h}^{\mathrm{FHNC/0}}(\mathbf{r}_1,\mathbf{r}_2,\mathbf{r}_{1'})$ as a function of r_{12} for fixed values of $r_{11'}$ (less than ~ 3 fm) and of θ (not small), one sees a rapid increase with r_{12}, toward the asymptotic behavior prescribed by Eq. (8). When $\rho_{2h}^{\mathrm{FHNC/0}}$ is viewed instead as a function of $r_{11'}$ for fixed values of r_{12} and θ, it exhibits oscillatory behavior. These behaviors are dictated mainly by the first term in the expression (14), namely $\rho\rho_1(r_{11'})g_{Qdd}(r_{12})g_{Qdd}(r_{1'2})$, which is the dominant contribution under the stated conditions.

The impact of the dynamical short-range correlations is revealed by comparing the plots in Figs. 2–5 derived from our FHNC/0 calculation with those for the ideal Fermi gas. Generally, the dynamical short-range correlations tend to

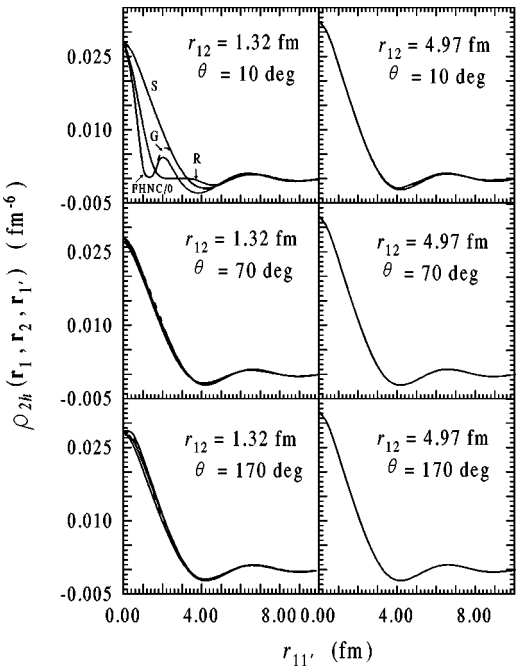

FIG. 7. Approximations $\rho_{2h}^{G}(\mathbf{r}_1,\mathbf{r}_2,\mathbf{r}_{1'})$ (dashed line G), $\rho_{2h}^{S}(\mathbf{r}_1,\mathbf{r}_2,\mathbf{r}_{1'})$ (solid line S), $\rho_{2h}^{R}(\mathbf{r}_1,\mathbf{r}_2,\mathbf{r}_{1'})$ (solid line R), and $\rho_{2h}^{\mathrm{FHNC/0}}(\mathbf{r}_1,\mathbf{r}_2,\mathbf{r}_{1'})$ (solid line FHNC/0), for the MC model of uniform symmetrical nuclear matter, as functions of $r_{11'}$, for representative values of r_{12} and $\theta\equiv\widehat{(\mathbf{r}_{11'},\mathbf{r}_{12})}$. (For $r_{12}=1.32$ fm and $\theta=70°$, 170° and for $r_{12}=4.97$ fm, the four curves are essentially indistinguishable.)

lower the values of ρ_{2h}, and this effect is seen to be quite pronounced.

IV. NUMERICAL COMPARISON WITH APPROXIMATIONS OF GERSCH *et al.*, SILVER, AND RINAT

It is of practical interest to compare the predictions of the simple formulas (9)–(11) for $\rho_{2h}(\mathbf{r}_1,\mathbf{r}_2,\mathbf{r}_{1'})$ with the results of the FHNC/0 evaluation of this quantity. As inputs for $g(r)$ and $\rho(\mathbf{r}_1,\mathbf{r}_{1'})$ in the constructions (9)–(11), we take the FHNC/0 versions of these quantities calculated for the MC model. Figures 6–8 illustrate the comparison for selected values of the variables $r_{11'}$, r_{12}, and $\theta\equiv\widehat{(\mathbf{r}_{11'},\mathbf{r}_{12})}$. It should be noted that $\rho_{2h}^{S}(\mathbf{r}_1,\mathbf{r}_2,\mathbf{r}_{1'})$ does not depend on the variable $r_{1'2}$ or θ. In Fig. 6, we display $\rho_{2h}(\mathbf{r}_1,\mathbf{r}_2,\mathbf{r}_{1'})$ as a function of r_{12} for nine combinations of values of the variables $r_{11'}$ (0.10, 1.93, and 4.97 fm) and θ (10°, 70°, and 170°). Similarly, in Fig. 7, ρ_{2h} is plotted as a function of $r_{11'}$ for six combinations of values of the variables r_{12} (1.32 and 4.97 fm) and θ (10°, 70°, and 170°). Finally, Fig. 8 presents results for ρ_{2h} as a function of θ for six combinations of values of $r_{11'}$ (0.10, 1.93, and 4.97 fm) and r_{12} (1.32 and 4.97 fm).

The behaviors of $\rho_{2h}^{\mathrm{FHNC/0}}$, ρ_{2h}^{G}, and ρ_{2h}^{R} as functions of r_{12} at given $r_{11'}$, and as functions of $r_{11'}$ at given r_{12}, depend on the value of θ, whereas the behavior of the approximation ρ_{2h}^{S} is independent of θ. As can be seen mainly from Figs. 6 and 7, ρ_{2h}^{R} and ρ_{2h}^{S} show the most prominent deviations from $\rho_{2h}^{\mathrm{FHNC/0}}$ at small values of θ (and not very small values of $r_{11'}$), for all values of r_{12}. On the other hand, ρ_{2h}^{G} remains rather close to $\rho_{2h}^{\mathrm{FHNC/0}}$. For intermediate

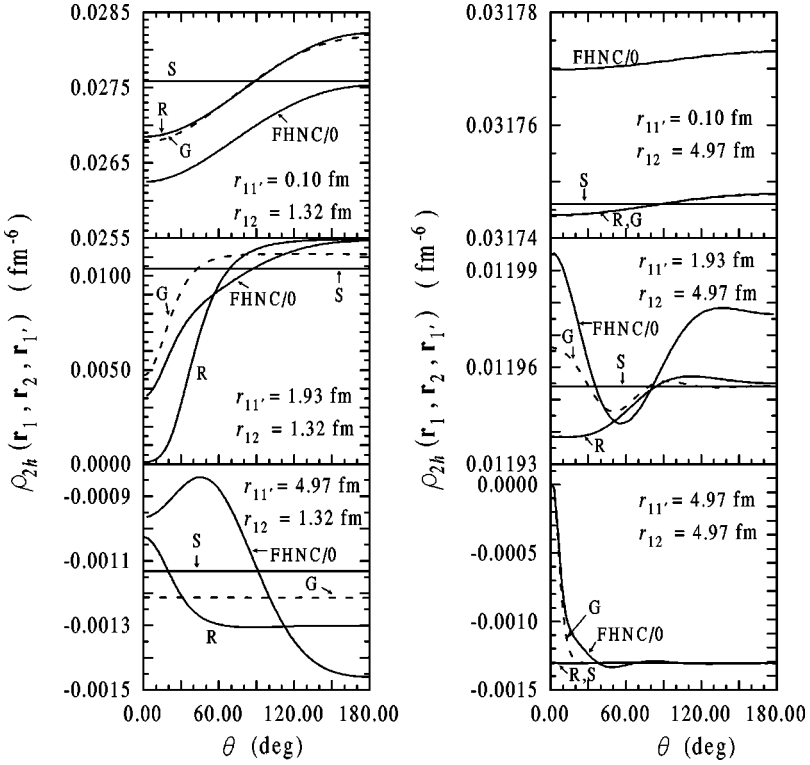

FIG. 8. Approximations $\rho_{2h}^{G}(\mathbf{r}_1,\mathbf{r}_2,\mathbf{r}_{1'})$ (dashed line G), $\rho_{2h}^{S}(\mathbf{r}_1,\mathbf{r}_2,\mathbf{r}_{1'})$ (solid line S), $\rho_{2h}^{R}(\mathbf{r}_1,\mathbf{r}_2,\mathbf{r}_{1'})$ (solid line R), and $\rho_{2h}^{\mathrm{FHNC/0}}(\mathbf{r}_1,\mathbf{r}_2,\mathbf{r}_{1'})$ (solid line FHNC/0), for the MC model of uniform symmetrical nuclear matter, as functions of $\theta\equiv\widehat{(\mathbf{r}_{11'},\mathbf{r}_{12})}$, for representative values of $r_{11'}$ and r_{12}.

and large values of θ (and again not very small values of $r_{11'}$), the approximation ρ_{2h}^{R} shows significant departures from $\rho_{2h}^{\mathrm{FHNC/0}}$, whereas ρ_{2h}^{S} and ρ_{2h}^{G} exhibit behavior similar to $\rho_{2h}^{\mathrm{FHNC/0}}$ (the similarity being greater for ρ_{2h}^{G}). Considering the three simple estimates, on the whole ρ_{2h}^{G} deviates least from $\rho_{2h}^{\mathrm{FHNC/0}}$; this rough agreement presumably stems from the fact that, within the FHNC/0 algorithm, the functions $[g(r)]^{1/2}$ (with $r=r_{12}$ or $r=r_{1'2}$) appearing in expression (9) behave in a manner similar to the functions $g_{Qdd}(r)$ appearing in the leading first term of the expression (14) for $\rho_{2h}^{\mathrm{FHNC/0}}$.

V. CONCLUSIONS

In summary, we have presented a microscopic evaluation, within Fermi hypernetted-chain theory, of the half-diagonal two-body density matrix of nuclear matter $\rho_{2h}(\mathbf{r}_1,\mathbf{r}_2,\mathbf{r}_{1'})$ for the case of state independent, central, two-body correlations. The momentum-space transform $n(\mathbf{p},\mathbf{Q})$ of ρ_{2h} has been studied previously in the same context [2,3]. Our results for ρ_{2h} demonstrate a rich sensitivity of this quantity to short-range correlations. The simple approximations to ρ_{2h} due to Silver and Rinat depart significantly from the FHNC/0 results in certain regions of the pertinent spatial variables, while such deviations are less prominent for the approximation of Gersch *et al.*

These results have immediate application within existing treatments of final-state interactions. Indeed, the FHNC/0 evaluation of ρ_{2h} has been employed as input to a description of FSI in inclusive quasielastic scattering of GeV electrons from nuclear matter, based on correlated Glauber theory, with findings to be detailed elsewhere [42]. Further studies of $\rho_{2h}(\mathbf{r}_1,\mathbf{r}_2,\mathbf{r}_{1'})$ in nuclear matter should extend the analysis and the calculations to realistic, state-dependent correlations. There have been some efforts in this direction within self-consistent Green's function theory [43]. As a first step toward microscopic determination of ρ_{2h} in finite nuclei, a local-density approximation may be developed, in analogy with what has been done for the one-body density matrix in Refs. [44,45].

[1] M. L. Ristig and J. W. Clark, Phys. Rev. B **41**, 8811 (1990).
[2] J. W. Clark, E. Mavrommatis, and M. Petraki, Acta Phys. Pol. **24**, 659 (1993) [Janusz Dabrowski Festschrift Issue].
[3] E. Mavrommatis, M. Petraki, and J. W. Clark, Phys. Rev. C **51**, 1849 (1995).
[4] H. A. Gersch, L. J. Rodriguez, and P. N. Smith, Phys. Rev. A **5**, 1547 (1972).
[5] R. N. Silver, Phys. Rev. B **38**, 2283 (1988).
[6] A. S. Rinat, Phys. Rev. B **40**, 6625 (1989).
[7] A. S. Rinat and M. F. Taragin, Nucl. Phys. **A571**, 733 (1994).
[8] J. W. Clark and R. N. Silver, in *Proceedings of the Fifth International Conference on Nuclear Reaction Mechanisms*, edited by E. Gadioli (Universitá degli Studi di Milano, Milano, 1988), p. 531.
[9] J. W. Clark, in *Progress in Particle and Nuclear Physics*, edited by D. H. Wilkinson (Pergamon, Oxford, 1979), Vol. 2, p. 89.
[10] M. A. Dal Ri, S. Stringari, and O. Bohigas, Nucl. Phys. **A376**, 81 (1982).
[11] A. Fabrocini (private communication).
[12] D. H. Beck, Phys. Rev. Lett. **64**, 268 (1990).
[13] S. Stringari, Phys. Rev. B **46**, 2974 (1992).
[14] F. Mazzanti, Ph.D. thesis, Universitat de Barcelona, 1997.
[15] E. A. J. M. Offermann, L. S. Cardman, H. J. Emrich, G. Fricke, C. W. de Jager, H. Miska, D. Rychel, and H. de Vries, Phys. Rev. Lett. **57**, 1546 (1986).
[16] O. Benhar, A. Fabrocini, S. Fantoni, G. A. Miller, V. R. Pandharipande, and I. Sick, Phys. Rev. C **44**, 2328 (1991).
[17] I. Sick, Prog. Part. Nucl. Phys. **34**, 323 (1995), and references therein.
[18] S. Boffi, C. Giusti, F. D. Pacati, and M. Radici, *Electromagnetic Response of Atomic Nuclei*, Oxford Studies in Nuclear Physics Vol. 20 (Clarendon, Oxford, 1996), and references therein.
[19] J. Arrington *et al.*, Phys. Rev. Lett. **82**, 2056 (1999).
[20] L. Lapikás, Nucl. Phys. **A553**, 297c (1993), and references therein.
[21] N. C. R. Makins *et al.*, Phys. Rev. Lett. **72**, 1986 (1994).
[22] T. G. O' Neill *et al.*, Phys. Lett. B **351**, 87 (1995).
[23] D. Abbott *et al.*, Phys. Rev. Lett. **80**, 5072 (1998).
[24] J. H. Morrison *et al.*, Phys. Rev. C **59**, 221 (1999).
[25] L. J. H. M. Kester *et al.*, Phys. Rev. Lett. **74**, 1712 (1995).
[26] K. I. Blomqvist *et al.*, Phys. Lett. B **421**, 71 (1998).
[27] C. J. G. Onderwater *et al.*, Phys. Rev. Lett. **81**, 2213 (1998).
[28] A. S. Carroll *et al.*, Phys. Rev. Lett. **61**, 1698 (1988).
[29] I. Mardor *et al.*, Phys. Rev. Lett. **81**, 5085 (1998).
[30] J. A. Eden *et al.*, Phys. Rev. C **44**, 753 (1991).
[31] P. D. Harty *et al.*, Phys. Rev. C **47**, 2185 (1993).
[32] J. R. Annand *et al.*, Phys. Rev. Lett. **71**, 2703 (1993).
[33] B. E. Andersson *et al.*, Phys. Rev. C **51**, 2553 (1995).
[34] P. D. Harty *et al.*, Phys. Rev. C **57**, 123 (1998).
[35] M. L. Ristig and J. W. Clark, Phys. Rev. B **40**, 4355 (1989).
[36] M. L. Ristig, in *From Nuclei to Particles*, Proceedings of the International School of Physics "Enrico Fermi," Course LXXIX, Varenna, 1980, edited by A. Molinari (North-Holland, Amsterdam, 1982), p. 340.
[37] S. Fantoni, Nuovo Cimento A **44**, 191 (1978).
[38] V. R. Pandharipande and R. B. Wiringa, Rev. Mod. Phys. **51**, 821 (1979).
[39] D. Ceperley, G. V. Chester, and M. H. Kalos, Phys. Rev. B **16**, 3081 (1977).
[40] M. F. Flynn, J. W. Clark, R. M. Panoff, O. Bohigas, and S. Stringari, Nucl. Phys. **A427**, 253 (1984).
[41] V. R. Pandharipande, R. B. Wiringa, and B. D. Day, Phys. Lett. **57B**, 205 (1975).
[42] M. Petraki, O. Benhar, J. W. Clark, A. Fabrocini, S. Fantoni, and E. Mavrommatis, in *Proceedings of the European Conference on Advances in Nuclear Physics and Related Areas, Thes-*

saloniki, Greece, 1997, edited by D. M. Brink, M. E. Grypeos, and S. E. Massen (Giahoudi-Giapouli Publishing, Thessaloniki, Greece 1999), p. 334; (to be published).
[43] C. C. Gearhart, Ph.D. thesis, Washington University, 1994.
[44] S. Stringari, M. Traini, and O. Bohigas, Nucl. Phys. **A516**, 33 (1990).
[45] G. Có, A. Fabrocini, and S. Fantoni, Nucl. Phys. **A568**, 73 (1994).